

Supplementary Materials

Deciphering the strength-ductility trade-off in (CuNiMn)-X alloys via interpretable machine learning

Fei Tan¹, Wei Chen¹, Zixuan Zhao¹, Yanbin Jiang^{1,2,*}, Meng Wang¹, Jiaqi Lan¹, Wenqin Xu¹, Zhu Xiao¹, Guofu Xu¹, Zhou Li¹

¹School of Materials Science and Engineering, Central South University, Changsha 410083, Hunan, China.

²State Key Laboratory for Powder Metallurgy, Central South University, Changsha 410083, Hunan, China.

***Correspondence to:** Prof. Yanbin Jiang, School of Materials Science and Engineering, Central South University, Changsha 410083, Hunan, China. E-mail: jiangyanbin@tsinghua.org.cn

Supplementary Table 1. Compositional boundaries of elements in the dataset used for model training

Elements	Atomic fraction range (at.%)	Number of entries	Frequency (%)	Category
Cu	0 - 33.33	500	37.3	Principal element in CuNiMn-X alloys
Ni	0 - 38.44	758	56.6	Principal element in CuNiMn-X alloys
Mn	0 - 33.33	458	34.2	Principal element in CuNiMn-X alloys
Al	0 - 42.86	617	46.0	X element for composition screening
Ti	0 - 37.50	511	38.1	X element for composition screening
Cr	0 - 40.00	657	49.0	X element for composition screening
Fe	0 - 40.00	676	50.4	X element for composition screening
Co	0 - 43.75	666	49.7	Other element in the dataset
V	0 - 50.00	514	38.4	Other element in the dataset
Mo	0 - 33.33	451	33.7	Other element in the dataset
Nb	0 - 30.30	443	33.1	Other element in the dataset
W	0 - 25.00	335	25.0	Other element in the dataset
Ta	0 - 25.00	354	26.4	Other element in the dataset
Hf	0 - 25.00	148	11.0	Other element in the dataset
Zr	0 - 37.50	174	13.0	Other element in the dataset
Si	0 - 20.00	21	1.6	Other element in the dataset
Sn	0 - 11.11	13	1.0	Other element in the dataset

Note: The atomic fraction range was obtained by normalizing the nominal alloy formula ratios. The “Number of entries containing this element” indicates the number of alloy compositions in which the corresponding element appears. The frequency was calculated as the number of entries containing the element divided by the total number of dataset entries, i.e., 1,340. Since this table reports elemental occurrence rather than mutually exclusive compositional systems, the sum of frequencies exceeds 100%.

Supplementary Table 2. Phase-type distribution of the dataset used for model training

Phase type	BCC	FCC	BCC + FCC
Number of entries	595	495	250
Proportion (%)	44.4	36.9	18.7

Note: Phase labels were assigned according to the phase information reported in the original literature. The proportion was calculated as the number of entries in each phase category divided by the total number of dataset entries.

Supplementary Table 3. Statistical performance of the models over 100 independent random train/test splits

Target	Optimal accuracy (%)	Mean R ² (%)	Standard deviation (%)
SVR - Strength	89.2	83.9	2.41
RFR - Strength	83.9	72.0	6.01
SVR - Fracture strain	88.1	82.6	1.85
RFR - Fracture strain	80.8	73.6	7.38

For the phase-type prediction model, the output was treated as a multi-class classification problem, including BCC, FCC, and BCC+FCC phases. Therefore, in addition to the overall prediction accuracy, precision, recall, and F1-score were calculated to evaluate the classification performance more comprehensively. The F1-score was defined as the harmonic mean of precision and recall:

$$Precision = \frac{TP}{TP + FP} \quad (1)$$

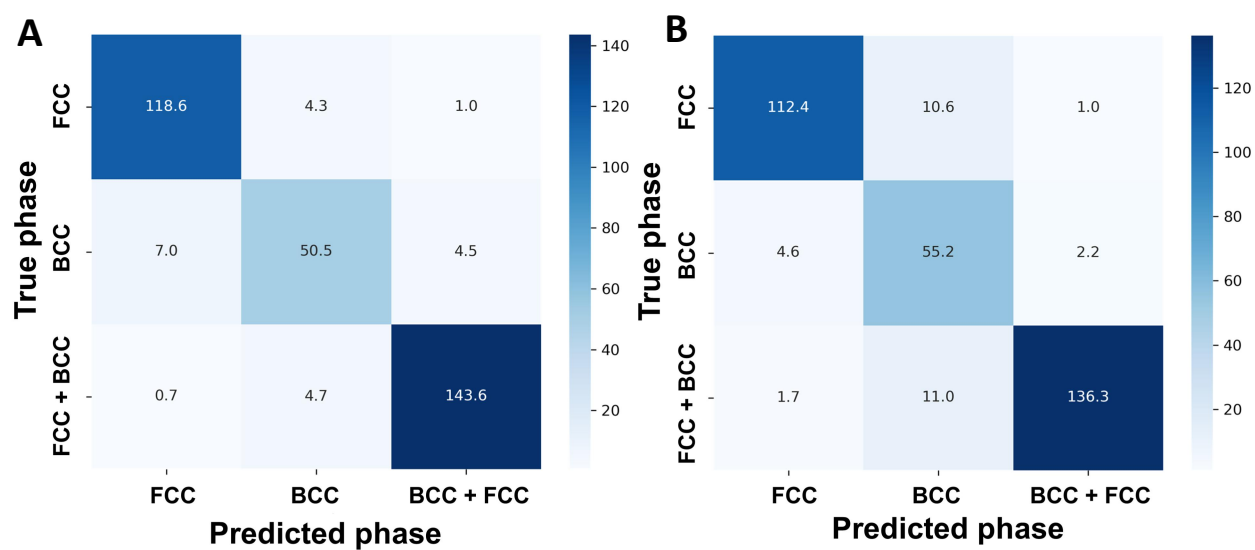
$$Recall = \frac{TP}{TP + FN} \quad (2)$$

$$F1 = \frac{2 \times Precision \times Recall}{Precision + Recall} \quad (3)$$

where TP , FP , and FN represent true positives, false positives, and false negatives, respectively. For the multi-class phase classification task, precision, recall, and F1-score were calculated for each phase category, and macro-average and weighted-average values were further reported. A confusion matrix was also constructed to visualize the classification performance among BCC, FCC, and BCC+FCC phases.

Supplementary Table 4. Classification performance of the phase prediction model

Phase model	Accuracy	Precision	Recall	Macro F1- score	Weighted F1 - score
SVC	92.34±1.19%	91.75±1.58%	91.14±1.83%	91.37±1.63%	93.29±1.22%
RFC	90.70±1.69%	88.21±1.83%	90.36±1.72%	88.88±1.88%	91.02±1.56%



Supplementary Figure 1. Confusion matrix of the Random Forest (A) and SVM-RBF (B) phase classification model for FCC, BCC, and BCC+FCC phases.